International Journal of Research in Engineering and Science (IJRES)
ISSN (Online): 2320-9364, ISSN (Print): 2320-9356
www.ijres.org Volume 9 Issue 9 ǁ 2021 ǁ PP. 71-80

Improving Efficiency of PEMFC based Electric Vehicle by using the Techniques of NN based MPPT controller

Pranali Surendra Kawle[1], Dr. Manisha V. Jape [2]
[*1]*M-Tech Student, Electrical Power System, Department of Electrical Engineering,*
kawlepranali023@gmail.com Government College of Engineering,
Amravati, India
[2]*Assistent Professor, Electrical Power System, Department of Electrical Engineering, manishajape@gmail.com*
Government College of Engineering,
Amravati, India

Abstract- *As a result of stricter regulations on carbon emissions and fuel economy, Fuel Cell Electric Vehicles (FCEV) are becoming increasingly popular in the automotive industry. This paper introduces the Maximum Power Point Tracking (MPPT) controller with neural network (NN) of the 1.26 kW Proton Exchange Membrane Fuel Cell (PEMFC) which provides drivetrain electric vehicles of DC-DC step-up converter. MPPT controller with Neural Network (NN) utilizes the Radial Basis Function Network (RBFN) for tracking the maximum power of the PEMFC. High divert frequency and high DC-DC converting power is important for the continuation of FCEV. The three-phase power supply Interleaved Boost Converter (IBC) is also designed to gain the maximum amount of power for the FCEV system. The interleaving technique reduces the ripple current, ripple voltage, and power pressure on the semiconductor power devices. FCEV framework execution examination with RBFN based MPPT control contrasted with Fuzzy Logic Controller (FLC) on the MATLAB/Simulink stage.*
Keywords*: Fuel cell electric vehicle, high voltages gain IBC, PEMFC, MPPT, RBFN, etc.*

Date of Submission: 26-08-2021 Date of acceptance: 10-09-2021

I. INTRODUCTION

Due to the environmental pollution and finite reserves of fossil fuels, automobile industries are showing more interest in electric cell electric vehicles (FCEV). The fast evaluations in power electronics and fuel cell technologies have allowed numerous developments in FCEVS. Fuel cells have the advantages of fresh energy production, high reliability, high performance, and low sound. Cells are categorized into different classes like proton exchange membrane fuel cells (PEMFC), alkaline fuel cells (AFC), oxyacid fuel cells (PAFC), solid oxide cells (SOFC), and molten carbonate electric cells (MCFC). PEMFC seems to be highly preferable over other types, mainly because of their reduced operating temperature, quick start-up times, and thermal management issues. In MPPT techniques, P&O is simple, popular, and straightforward to use. P&O and incremental conduction both caused oscillations at a steady state which may reduce the efficiency of the fuel cell system. To overcome this problem, symbolic logic controllers and neural network algorithms were introduced to detect MPPT with increased efficiency and accuracy. Radial basis function network (RBFN) MPPT base control suggested PEMFC MPPT tracking. A high voltage gains a three-phase non-isolated interleaved boost converter (IBC) for electric cell applications to achieve low switching stress and high voltage gain. The fraudulent measures the reliability of the cell and provides greater power. The output voltage of the proposed converter is given to the electrical motor through an inverter for the propulsion of the vehicle. The electrical motor plays a vital role in FCEVs. An adequate motor considerably reduces the price and size of the cell.

A boost converter is extensively used as a front-end power conditioner for the cell. For low power applications, the standard boost converter is employed as an influence electronic interface whereas for prime power applications boost converter won't be compatible thanks to its low current handling capability and thermal management issues. To beat these problems different high voltage, gain DC-DC converters are designed. Isolated converters with coupled inductors or high-frequency transformers are proposed to attain high voltage gain. The maximum gain in power is obtained by adjusting the converter rate. However, these single converters are more attractive compared to DC-DC converters that are not isolated. So, this project proposes a high voltage gain three-phase non-isolated interleaved boost converter (IBC) for electric cell applications to achieve low switching stress and high voltage gain. The Interleaving method builds the unwavering quality of the electric cell and gives high force capacity. The output voltage of the proposed converter is given to the electrical motor through an inverter for the propulsion of the vehicle. The electrical motor plays a crucial role in FCEVs. An adequate motor considerably reduces the value and size of the cell. In past, the bulk of automakers

are used DC motors for electric vehicle applications. Adversely, DC motors have high maintenance cost and low efficiency because of the brushes and rotating devices.

A quadratic boost converter composed of two boost converters is proposed to realize high voltage gain. But by using two boosts converter may reduce the overall efficiency of the vehicle. A 2-phase flexible converter amplified between DC-DC protective is recommended. However, this topology suffers from poor reliability and lower efficiency. In, a lift converter with a voltage multiplier cell is proposed to realize high voltage gain, but the voltage gain of a single multiplier cell isn't much enough to drive the ability train of FCEV. The Conventional configuration gives some advantages of poor reliability, less efficiency, and highly expensive so to overcome this problem DC-DC converters are used. This paper presents that high voltage acquired of three to Single-phase interleaved boost converter (IBC) of fuel cell for low switching stress and high voltage gain. The NN-based MPPT controller is used to save time increases the reliability of the fuel cell and provides high power of Fig 2 Displays the proposed BLDC. FCEV of IBC with a higher level. It included 1.26 KW of PEMFC, an IBC with a 3-phase high-voltage gain, a voltage source inverter (VSI), and a BLDC motor. The interleaved boost converter (IBC) distributes as an interface between FC and VSI. The RBFN is designed to deliver high power to a fuel cell. The IBC provides power to the BLDC through VSI. Switches of the VSI are controlled by using the electronic commutations of the BLDC motor. The motor shaft is connected to the wheels for the propulsion.

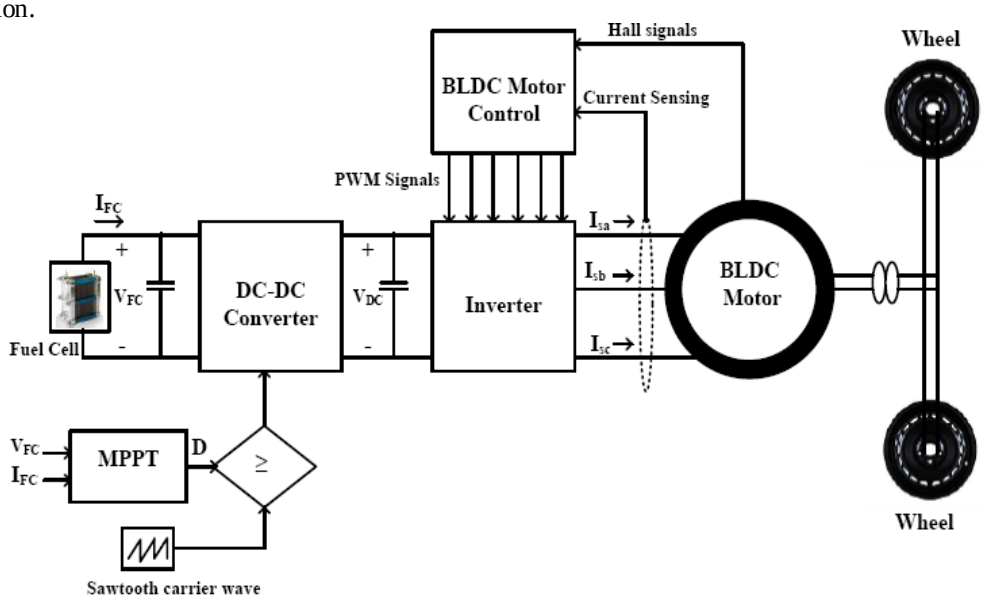

Fig 1 Conventional configuration of fuel cell provides BLDC motor-driven electric vehicle.

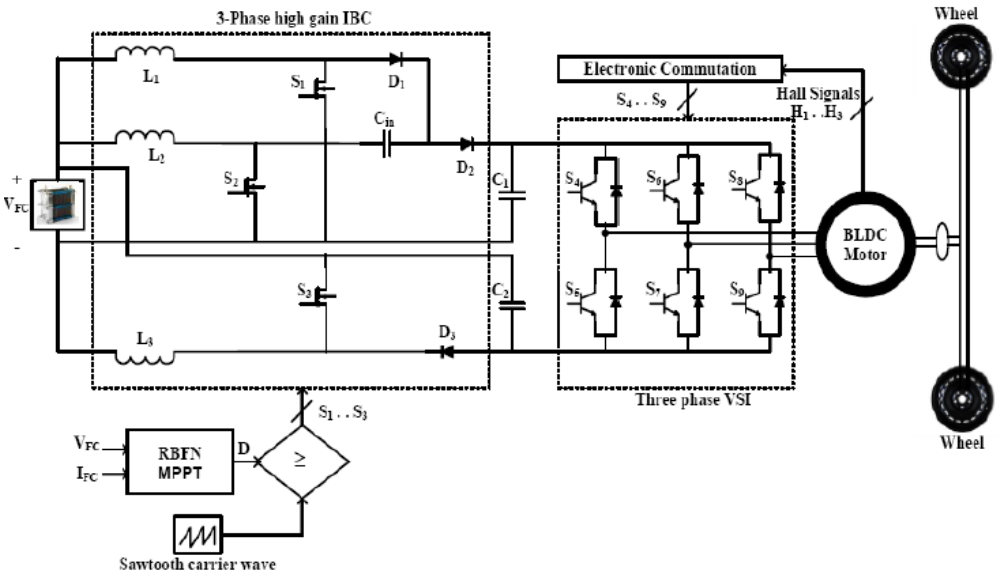

Fig 2 Advanced BLDC motor driven FCEV system with three-phase high voltage gain IBC

II. FUEL CELL MODELING

As a result of electrochemical reaction fuel cell is converted hydrogen fuel into electricity. The inputs of the fuel cell are air these are converted into water and electricity. A single fuel cell consists of two electrodes and an electrolyte. The electrolyte separates the positive and negatives a charged ion of the hydrogen fuel. When hydrogen and oxygen are provided into the cell, electricity is generated at the output of the cell in the presence of an electrolyte. A fuel cell produces only heat and water as the wastage of the chemical reaction Electrolyte. A Fuel cell produces only heat and water as the wastage of the chemical reaction. The input voltage PEMFC is given as,

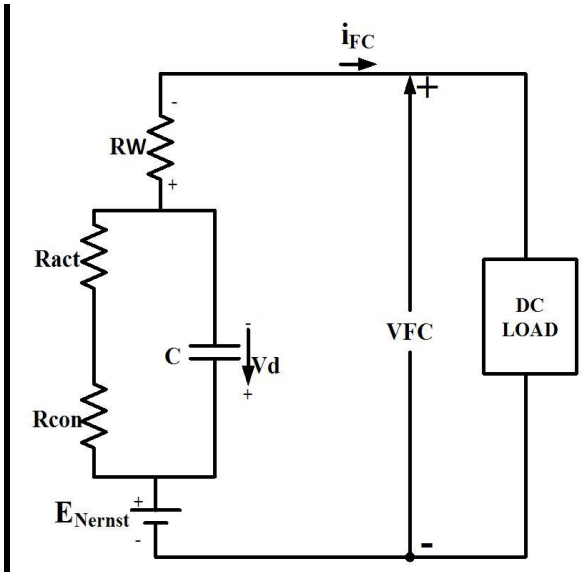

Fig.3 Electric model of (PEMFC)

The cell voltage of PEMFC is given as,

$V_{FC}= E_{Nernst} -V_{act} -V_{ohm} -V_{con}$ (1)

Where N_{ernst} is the open-circuit (or reversible) thermodynamic voltage and is given as,

E_{nerst}=1.229 -8.5×10^{-4}(T-298.15)+4.308×10^{-5}T($l_n(P_{H2}) + 0.5l_n(P_{O2})$) (2)

Where T is the absolute temperature (K), P_{O2} and P_{h2} is oxygen and hydrogen partial pressures respectively.

Activation voltage V_{act} is the combination of both anode and cathode activation over voltage and is expressed as,

V_{act}= -[$\partial_1 + \partial_2 T + \partial_3 T l_n(C_{O2}) + \partial_4 T l_n(I_{FC})$] (3)

Where,

I (I= 1, 2, 3, 4) is empirical coefficient for each cell and C_{O2} is the dissolved oxygen concentration at the liquid/gas interface and is calculated by using the following expression,

$C_{O2} = \frac{P_{O2}}{(5.08\times10^6)\times\exp(-\frac{498}{T})}$ (4)

V_{Ohmic} Over voltage V_{ohm} is expressed as,

$V_{ohm} = I_{FC}\,(R_C + R_M)$ (5)

Where $R_M$the electron is flow equivalent resistance and R_C is the proton resistance. R_C Is considered as constant

$R_M = \frac{\rho_m L}{A}$ (6)

Where L is membrane thickness (cm), Denotes active area of membrane (Cm^2) and m is the membrane specific resistivity (Ω-cm) and is given as,

$\rho_m = \frac{181.6[1+0.03J+0.062\left(\frac{T}{303}\right)^2(J)2.5]}{[G-0.634-3J]\exp[4.18\left(1-\frac{303}{T}\right)]}$ (7)

Where G is the water content of the membrane and J is the current density and is expressed as,

$J=\frac{I_{FC}}{A}$ (8)

Finally, the concentration overvoltage V_{con} can be calculated from the following expression,

$V_{Con} = -\frac{RT}{nF} l_n(1 - \frac{J}{J_{max}})$ (9)

Where, F is Faraday's constant; R is universal gas constant and J_{max} is maximum current density.

PEMFC produces an unregulated low DC output voltage. Therefore a boost or step-up DC-DC converter is required to boost and regulate the PEMFC output voltage. A DC-DC converter is connected to the output of the

fuel cell to keep up a constant voltage across the DC link. The Proton Exchange Membrane Fuel Cell (PEMFC) parameters as shown in Table 1

TABLE 1 1.26 kW PEMFC parameter specifications

Parameter Description	Ratings
Maximum power (P_{max})	1.26 kw
Maximum current (I_{max})	52 A
Maximum voltage (V_{max})	24.23 V
Temperature (T)	55^0C
Number of cells	42
Nominal air flow rate	2400 IPM

III. Three-Phase High Voltage Gain IBC

The proposed converter consists of three switches (S_1, S_2 and S_3) and three diodes ($D_1, D_2$and D_3). $L_1, L_2$and L_3 Are the filtering inductors of one phase, two phases and three-phase respectively, V_{FC} is the input voltage, V_0 is output voltage and R is the load resistor. The following assumptions are observed for the analysis of the proposed high voltage gain IBC:

i. Inductors of all three phases are assumed to be ideal ($L_1 = L_2 = L_3$=L).
ii. Filtering capacitors C_1 and $C_2$are considered assume ($C_1 = C_2$=C).
iii. The proposed converter always used in Continuous Conduction Mode (CCM).

The voltage and current ripples across the capacitor and inductor are assumed to be very small. The switches S_1, S_2 and S_3 are switched ON by using two gate pulses which are 180˚ phase shifted. One pulse is given to the switch S_2 and another gate pulse with 180˚ phase shift is given to both the switches S_1 andS_3. Fig bellow explains the operation of the proposed converter in different operating modes.

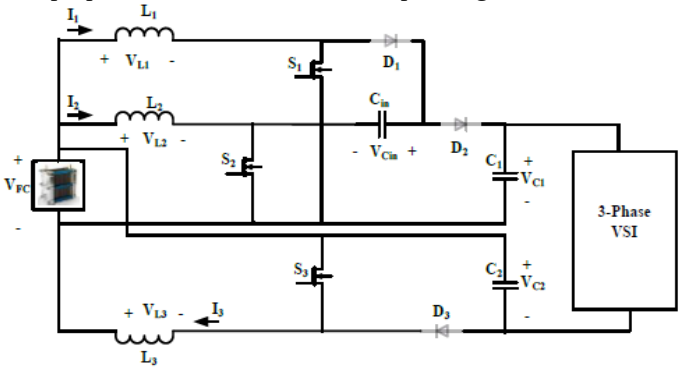

Fig 4(a) Modes of operation of 3-phase high voltage gain IBC

Mode-1 ($t_0 \le t \le t_1$): During this mode, all the three switches S_1, S_2 and S_3 are switched ON and all the three diodes D_1, D_2 and D_3 are reverse biased as shown in Fig. 3 (a). The input voltage source Vicarages the inductorsL_1, L_2 and L_3. The current through these inductors I_1, I_2 and I_3 increased linearly with a slope of (V_{FC}/L). The input capacitor Can is disconnected from the load as well as from the supply. The output capacitors C_1 and C_2 supplies energy to the load resistor and the voltage of output capacitors V_{C1} and V_{C2} decreases with a slope of (-V_0/R_C)

Mode-2 ($t_1 \le t \le t_2$): In this mode, the switch S_2 is switched ON and the switches S_1 and S_3 are switched OFF. The diodes $D_1$and D_3 are forward biased and the diode D_2 is reverse biased as shown in Fig. 4(b). The current through the inductors L_1 and L_3decreased with a slope of (V_{FC} –V_{Cin})/L and (V_{FC} –V_{C2})/L respectively. The current through the inductor L_2 increases with a slope of (V_{FC}/L). The capacitor C_1 supplies the energy to the load and the capacitors $C_2$and C_{in} is charged by the input voltageV_{FC}.

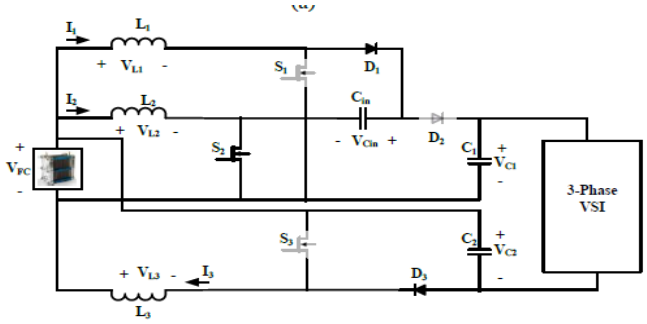

Fig 4(b) Modes of operation of 3-phase high voltage gain IBC

Mode-3 ($t_3 \leq t \leq t_4$): This mode is similar to mode-1. All the three switches S_1, S_2 and S_3 are switched ON and all the three diodes D_1, D_2 and D_3 are switched OFF.

Mode-4 ($t_4 \leq t \leq t_5$): In this mode, the switch S_2 is switched OFF and the switches S_1 and S_3 are switched ON. The diodes D_1 and D_3 are reverse biased and the diode D_2 is conducting as shown in Fig. 4(c). The input voltage source V_{FC} charges the inductors L_1 and L_3 the current through these inductors increases with a slope of (V_{FC}/L). The current through the inductor L_2 decreases with a slope of $(V_{FC}+V_{Cin}-V_{C1})/L$. The capacitors $C_2$and energy to the load. Capacitor C_1 gets charged by the input voltageV_{FC}.

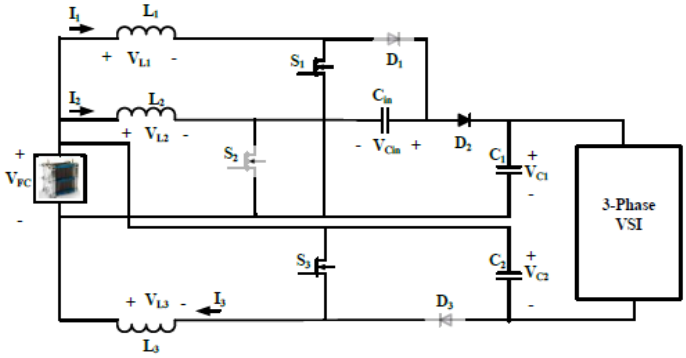

Fig. 4(c) Modes of operation of 3-phase high voltage gain IBC

IV. SIMULATION MODEL AND RESULTS ANALYSIS

The performance of the proposed BLDC motor driven FCEV system is analyzed by using the MATLAB/SIMULINK platform. To analyses the dynamic response of the FCEV system, sudden changes in the temperature of the fuel cell is considered as follows: T= 320˚k for a period of 0 to 0.3sec, T= 310˚k for a period of 0.3 sec to 0.6 sec and T= 330˚k for a period of 0.6sec to 0.9 sec.

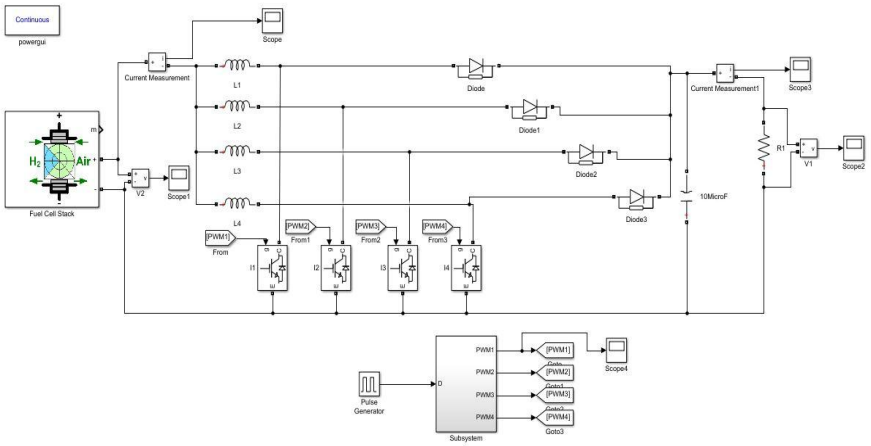

fig 5 simulation designed module of proposed system.

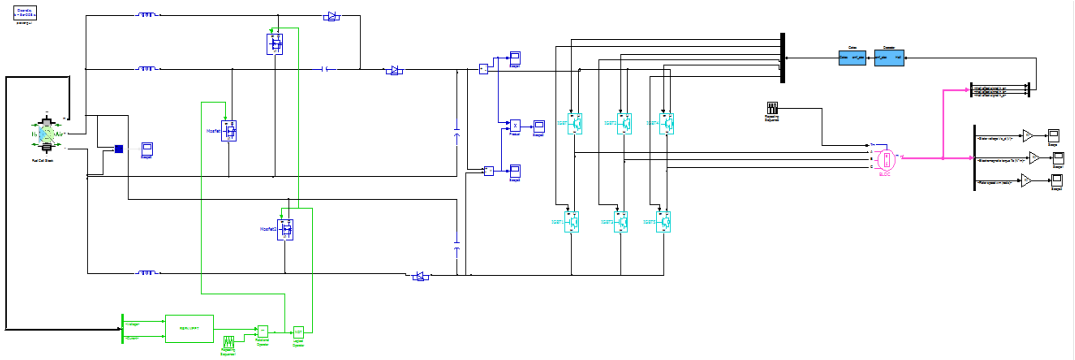

Fig 6 Simulation architecture of proposed system

The output voltage of fuel cell stack at different temperatures is shown in fig 7, fuel cell generates a voltage is around 200 volts to 188 volts this is fuel cell output voltage at the temperature of 320 degree kelvin, 310 degree kelvin, and 330 degree kelvin. The DC link output current, voltage and power using proposed RBFN based MPPT controller against the temperature of 320 degree kelvin, 310 degree kelvin, and 330 degree kelvin Shown in (fig 8, 9, 10,).

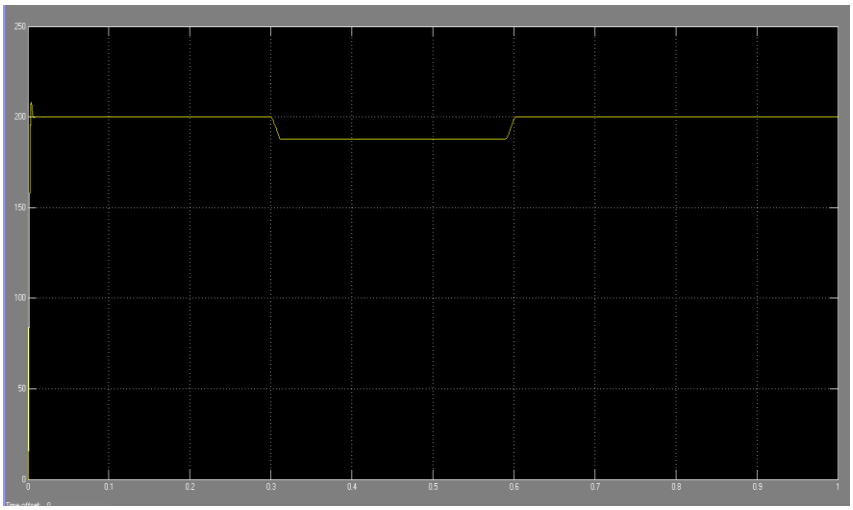

Fig 7 Output Voltage of Fuel Cell Stacks

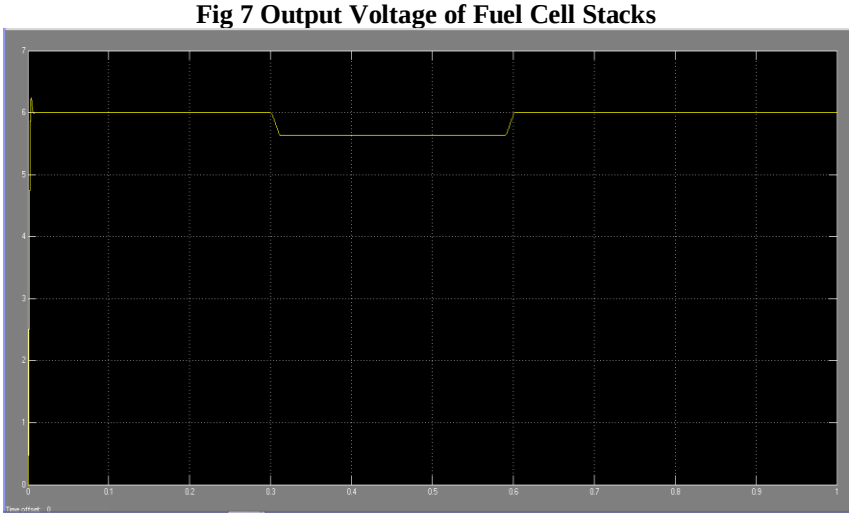

Fig 8 Output current of DC-DC converter at different temperatures using RBFN

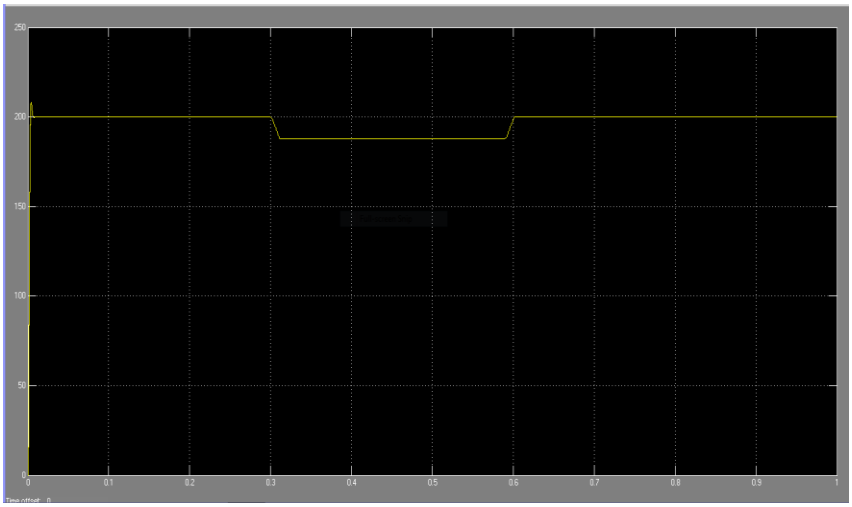

Fig 9 Output voltage of DC-DC converter at different temperatures using RBFN

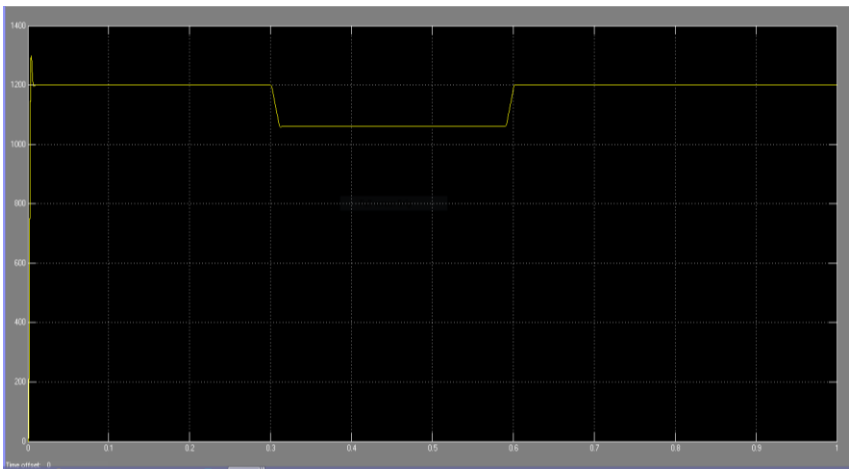

Fig 10 Output power of DC-DC converter at different temperatures using RBFN

A. BLDC parameters

The performance of the proposed BLDC motor-driven FCEV system is analyzed by using the Simulink platform. The DC link output current, voltage and power waveforms of the proposed controller using RBFN based MPPT controller with the temperature of T=320 degree kelvins for a time period of 0 to 0.3 sec, T=310 degree kelvin for a time period of 0 .3 to 0.6 sec, and T=330 degree kelvin for a time period of 0.6 to 0.9 sec. Fig11 shows the BLDC motor output power against temperature, Fig 12 shows the BLDC motor output electromagnetic torque against temperature; Fig 13 shows the BLDC motor output speed(RPM) against temperature.

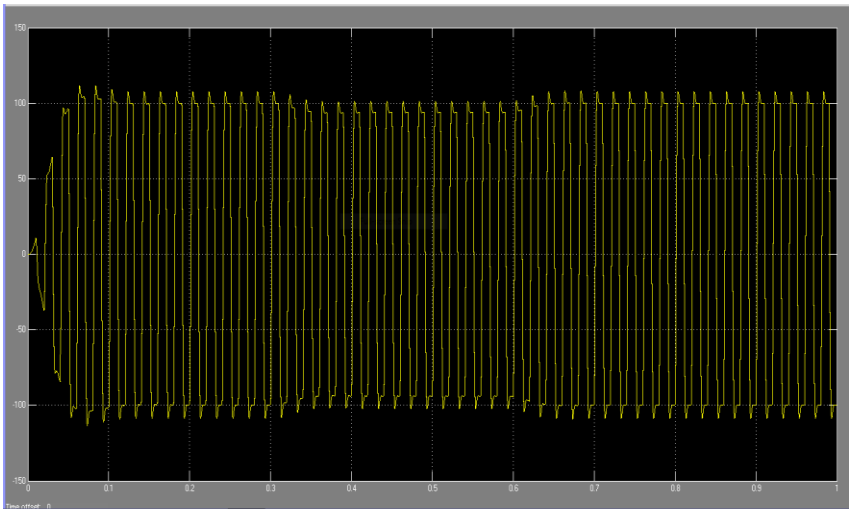

Fig 11 BLDC motor output power against temperature

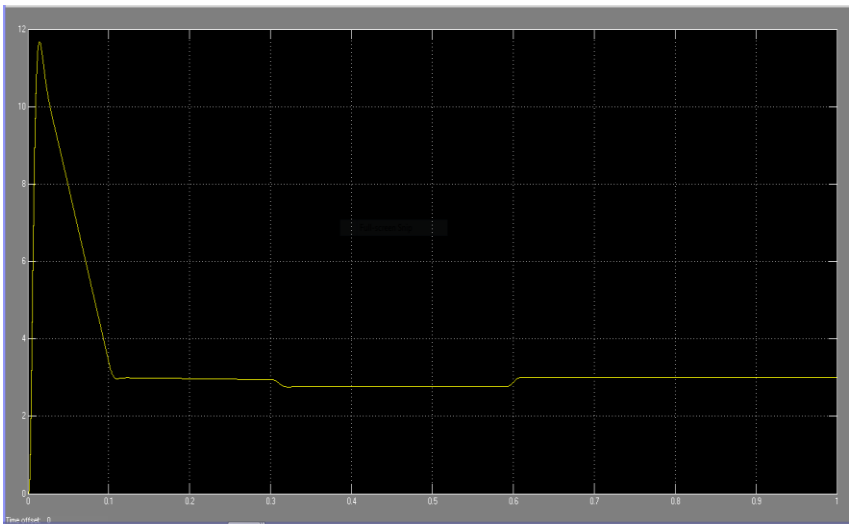

Fig 12 BLDC motor output electromagnetic torque against temperature

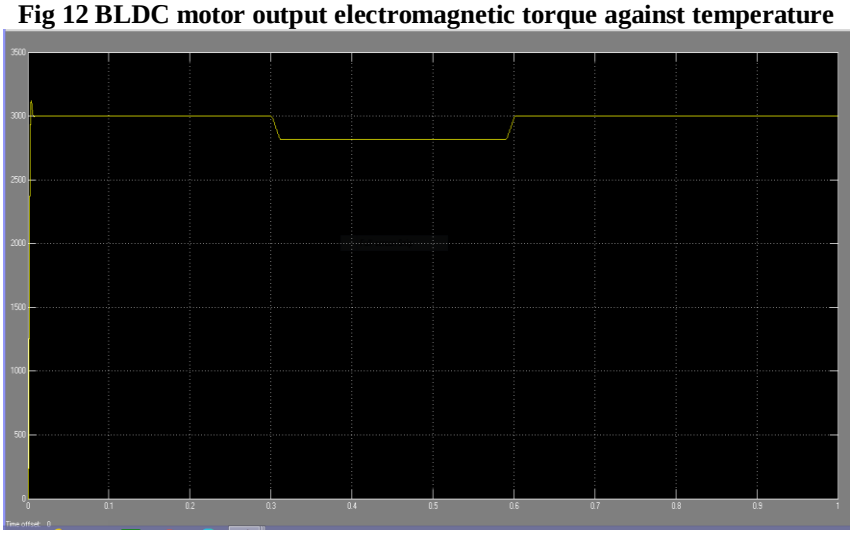

Fig 13 BLDC motor output speed (RPM) against temperature

V. Comparison of DC link power with both RBFN and Fuzzy based MPPT controllers

The performance of the RBFN based MPPT controller for fuel cell is compared with fuzzy logic based MPPT controller From Fig.14 it is observed that proposed controller generates the high DC link power than the FLC. The comparative analysis of 1.26 kW PEMFC with Fuzzy Logic Controller (FLC) based MPPT controller and 1.26 kW PEMFC with Radial Basis Function Network (RBFN) based MPPT Controller observed that the

RBFN controller is greater than the FLC it has listed in table 2 at the different temperature of 320 degree kelvin, 310 degree kelvin, and 330 degree kelvin. For time period of 0 to 0.3 sec, for a time period of 0.3 to 0.6 se , and for a time period of 0.6 to 0.9 sec.

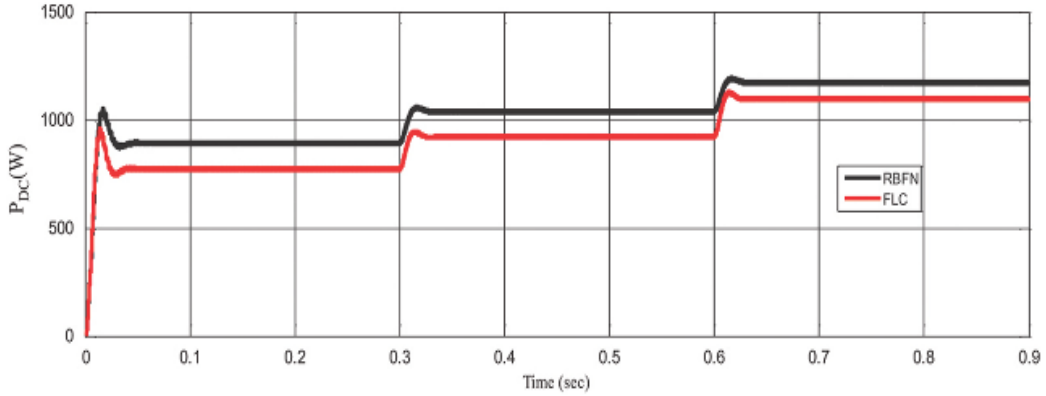

Fig 5.8 Comparison of DC link power with both RBFN and Fuzzy based MPP

TABLE 5.1 Comparison of DC link power with both RBFN and Fuzzy based MPPT controllers.

Parameter	1.26 kw PEMFC with fuzzy based MPPT			1.26 kw PEMFC with RBFN based MPPT		
Period(sec)	0 to 0.3	0.3 to 0.6	0.6 to0.9	0 to 0.3	0.3 to0.6	0.6 to0.9
Fuel cell temperature(degree)	320	310	330	320	310	330
DC link current(A)	4.71	4.2	5.1	4.8	4.4	5.21
DC link voltage(V)	193	188	210	200	193	220
DC link power(W)	1000	830	1150	1050	900	1200

VI. RESULTS AND DISCUSSION

The performance of the proposed BLDC motor-driven FCEV system is analyzed by using the Simulink platform. The DC link output current, voltage and power waveforms of the proposed controller using RBFN based MPPT controller with the temperature of T=320 degree kelvins for a time period of 0 to 0.3 sec, T=310 degree kelvin for a time period of 0 .3 to 0.6 sec, and T=330 degree kelvin for a time period of 0.6 to 0.9 sec, DC link voltage is 200 volt for a time period of 0 to 0.3 sec, 193 volt for a time period of 0.3 to 0.6 sec, and 220 volt for a time period of 0.6 to 0.9 sec. DC link current is 5 amp for a time period of 0 to 0.3 sec, 4 amp for a time period of 0.3 to 0.6 sec, and 6 amp for a time period of 0.6 to 0.9 sec. DC link power is 1050 watt for a time period of 0 to 0.3 sec, 900 watt for a time period of 0.3 to 0.6 sec, and 1200 watt for a time period of 0.6 to 0.9 sec. The BLDC motor parameters are like back EMF, electromagnetic torque, and speed of the motor are calculated at different temperature conditions of the fuel cell. The BLDC motor speed is 3300 rpm for a time period of 0 to 0.3 sec, 2400 rpm for a time period of 0.3 to 0.6 sec, and 3700 rpm for a time period of 0.6 to 0.9 sec. Torque of the BLDC motor is constant for varying speed of the motor

VII. CONCLUSION

The proposed system is designed for 1.26 kW power ratings. This designed system has been simulated using MATLAB/Simulink. Also, a three-phase high voltage gain DC-DC converter is proposed for FCEV applications. The proposed converter has reduced the fuel cell input current ripples and the voltage stress on the power semiconductor switches. The RBFN based MPPT technique is designed for 1.26 kW PEMFC for extracting the maximum power from the fuel cell at different temperatures. The RBFN based MPPT controller has compared with fuzzy based controller in comparison RBFN based MPPT controller has tracked the maximum power than fuzzy based controller. Also, different performance characteristics of the BLDC motor such as electromagnetic torque, speed and back EMF are evaluated at different temperatures of the fuel cell system.

REFERENCES

[1]. H.-J. Chiu and L.-W. Lin, ``A bidirectional DC-DC converter for fuel cell electric vehicle driving system," IEEE Trans. Power Electron., vol. 21, no. 4, pp. 950_958, Jul. 2006.

[2]. B. Geng, J. K. Mills, and D. Sun, ``Combined power management/design optimization for a fuel cell/battery plug-in hybrid electric vehicle using multi-objective particle swarm optimization," Int. J. Autom. Technol., vol. 15, no. 4, pp. 645_654, 2014.

[3]. H. Hemi, J. Ghouili, and A. Cheriti, ``A real-time fuzzy logic power management strategy for a fuel cell vehicle," Energy Convers. Manage., vol. 80, pp. 63_70, Apr. 2014.

[4]. N. Mebarki, T. Rekioua, Z. Mokrani, D. Rekioua, and S. Bacha, ``PEM fuel cell/battery storage system supplying electric vehicle," Int. J. Hydrogen Energy, vol. 41, no. 45, pp. 20993_21005, 2016.

[5]. S. Abdi, K. Afshar, N. Bigdeli, and S. Ahmadi, ``A novel approach for robust maximum power point tracking of PEM fuel cell generator using sliding mode control approach," Int. J. Electrochem. Sci., vol. 7, pp. 4192_4209, May 2012.

[6]. T. Esram and P. L. Chapman, ``Comparison of photovoltaic array maximum power point tracking techniques," IEEE Trans. Energy Convers., vol. 22, no. 2, pp. 439_449, Jun. 2007.

[7]. S. Saravanan and N. R. Babu, ``Maximum power point tracking algorithms for photovoltaic system_A review," Renew. Sustain. Energy Rev., vol. 57, pp. 192_204, May 2016.

[8]. J. P. Ram, N. Rajasekar, and M. Miyatake, ``Design and overview of maximum power point tracking techniques in the wind and solar photovoltaic systems: A review," Renew. Sustain. Energy Rev., vol. 73, pp. 1138_1159, Jun. 2017.

[9]. L. N. Khanh, J.-J. Seo, Y.-S. Kim, and D.-J. Won, ``Power-management strategies for a grid-connected PV-FC hybrid system," IEEE Trans. Power Del., vol. 25, no. 3, pp. 1874_1882, Jul. 2010.

[10]. A. Giustiniani, G. Petrone, G. Spagnuolo, and M. Vitelli, ``Low-frequency current oscillations and maximum power point tracking in grid-connected fuel-cell-based systems," IEEE Trans. Ind. Electron., vol. 57, no. 6, pp.